Environ. Sci. Technol. **1999**, *33,* 3586−3595

Products of the Gas-Phase Reactions of 1,3-Butadiene with OH and NO_3 Radicals

ERNESTO C. TUAZON,
ALVARO ALVARADO,[†]
SARA M. ASCHMANN,
ROGER ATKINSON,*[,‡,§] AND
JANET AREY*[,‡]
Air Pollution Research Center, University of California, Riverside, California 92521

1,3-Butadiene is emitted into the atmosphere from a number of sources including combustion sources and is listed in the United States as a hazardous air pollutant. In the atmosphere, 1,3-butadiene reacts with OH radicals, NO_3 radicals, and O_3 with the dominant tropospheric removal processes being daytime reaction with the OH radical and nighttime reaction with the NO_3 radical. We have used gas chromatography, in situ Fourier transform infrared (FT-IR) absorption spectroscopy, and in situ atmospheric pressure ionization tandem mass spectrometry (API-MS) to identify and quantify the products formed from the reactions of 1,3-butadiene with OH radicals (in the presence of NO) and NO_3 radicals. Acrolein, formaldehyde, and furan were identified and quantified from the OH radical-initiated reaction, with formation yields of 0.58 ± 0.04, 0.62 ± 0.05, and 0.03−0.04, respectively. Organic nitrates were observed by FT-IR spectroscopy with an estimated yield of 0.07 ± 0.03, and the API-MS analyses indicated that these organic nitrates are mainly the hydroxynitrate $HOCH_2CH{=}CHCH_2ONO_2$ and/or its isomers. API-MS analyses showed the formation of a hydroxycarbonyl with the formula $C_4H_6O_2$, attributed to $HOCH_2CH{=}CHCHO$ and/or its isomers. The major products of the NO_3 radical-initiated reaction were organic nitrates; the API-MS analyses indicated the formation of acrolein, 1,2-epoxy-3-butene, and unsaturated C_4-hydroxycarbonyls, hydroxynitrates, carbonyl nitrates, and nitrooxyhydroperoxides. Acrolein, HCHO, and furan were again quantified by gas chromatographic and FT-IR analyses. Our data are compared with previous literature studies, and detailed reaction mechanisms are presented and discussed.

Introduction

1,3-Butadiene [$CH_2{=}CHCH{=}CH_2$] is listed under Title III of the Clean Air Act Amendments of 1990 as a hazardous air pollutant (*1*) and is also on California's list of toxic air contaminants (*2*). 1,3-Butadiene is emitted into the atmosphere from a number of sources including vehicle exhaust (*3−10*) and tobacco smoke (*3, 11, 12*) and has been measured in the troposphere at various locations (*3, 13−19*). In the troposphere, 1,3-butadiene can undergo reaction with OH radicals, NO_3 radicals, O_3, and Cl atoms (*20*). By combining the rate constants for the OH radical, NO_3 radical, and O_3 reactions with estimated ambient concentrations of these reactive species, it is calculated that the daytime OH radical and nighttime NO_3 radical reactions are important transformation processes and that 1,3-butadiene typically has a lifetime in the troposphere of a few hours.

However, the products of the gas-phase reactions of 1,3-butadiene with OH and NO_3 radicals are not fully understood (*20−22*). The formation of HCHO and acrolein have been observed from the OH radical-initiated reaction of 1,3-butadiene (*23−25*) together with furan in 4−6% yield (*24, 26*). However, there is significant disagreement between the studies of Maldotti et al. (*23*) and Ohta (*24*) concerning the acrolein formation yield, with values of 98 ± 12% and ∼40%, respectively, being reported for reactions carried out in the presence of NO. For the NO_3 radical reaction, Barnes et al. (*27*) used in situ Fourier transform infrared (FT-IR) spectroscopic analyses and reported the formation of HCHO, acrolein, and organic nitrates with yields of 12%, 12%, and ∼60%, respectively. Skov et al. (*28*) also used in situ FT-IR spectroscopy to investigate the reactions of the NO_3 radical with 1,3-butadiene, 1,3-butadiene-1,1,4,4-d_4, and 1,3-butadiene-d_6 and concluded that terminal NO_3 radical addition dominated with the formation of *trans*-$O_2NOCH_2CH{=}CHCHO$ and $O_2NOCH_2C(O)CH{=}CH_2$ as the major products.

In this work, we have used gas chromatography, in situ FT-IR spectroscopy and in situ atmospheric pressure ionization tandem mass spectrometry (API-MS) to investigate the products and mechanisms of the gas-phase reactions of 1,3-butadiene with OH radicals (in the presence of NO) and NO_3 radicals. To aid in the identification of products, 1,3-butadiene-d_6 was also used in experiments employing API-MS for analyses.

Experimental Methods

Experiments were carried out at 298 ± 2 K and 740 Torr total pressure of air in a 5870-L evacuable, Teflon-coated chamber containing an in situ multiple reflection optical system interfaced to a Nicolet 7199 FT-IR spectrometer and with irradiation provided by a 24-kW xenon arc filtered through a 0.25 in. thick Pyrex pane (to remove wavelengths <300 nm); in a 7500-L Teflon chamber with analysis by gas chromatography with flame ionization detection (GC-FID) and combined gas chromatography−mass spectrometry (GC−MS), with irradiation provided by two parallel banks of black lamps; and in a 7300-L Teflon chamber interfaced to a PE Sciex API III MS/MS direct air sampling, atmospheric pressure ionization tandem mass spectrometer (API-MS), again with irradiation provided by two parallel banks of black lamps. All three chambers are fitted with Teflon-coated fans to ensure rapid mixing of reactants during their introduction into the chamber.

Hydroxyl radicals were generated in the presence of NO by the photolysis of methyl nitrite or ethyl nitrite in air at wavelengths >300 nm (*29, 30*):

$$RCH_2ONO + h\nu \rightarrow RCH_2\dot{O} + NO \quad (1)$$

$$RCH_2\dot{O} + O_2 \rightarrow RCHO + HO_2 \quad (2)$$

$$HO_2 + NO \rightarrow OH + NO_2 \quad (3)$$

where R = H or CH_3. NO was added to the reactant mixtures

---

* Corresponding authors.

[†] Present address: U.S. Environmental Protection Agency, Mail Code 3HS41, 1650 Arch Street, Philadelphia, PA 19103.

[‡] Also Department of Environmental Sciences, University of California, Riverside.

[§] Also Department of Chemistry, University of California, Riverside.

10.1021/es990193u CCC: $18.00

to suppress the formation of O_3 and hence of NO_3 radicals (*29*). Because HCHO is the major product from the photolysis of methyl nitrite in air, HCHO formation yields from the reaction of the OH radical with 1,3-butadiene were measured in experiments using ethyl nitrite photolysis as the source of OH radicals (*30*).

NO_3 radicals were generated by the thermal decomposition of N_2O_5 in the presence of NO_2 (*31, 32*):

$$N_2O_5 \rightarrow NO_3 + NO_2 \tag{4}$$

Teflon Chamber Experiments with GC-FID and GC−MS Analysis. For the OH radical reactions carried out in the 7500-L Teflon chamber (at ~5% relative humidity), OH radicals were generated by the photolysis of methyl nitrite in air, and the initial reactant concentrations (in molecule cm^{-3} units) were as follows: CH_3ONO, 2.0×10^{14}; NO, 1.9×10^{14}; and 1,3-butadiene, $(5.7{-}6.2) \times 10^{13}$. Irradiations were carried out at 20% of the maximum light intensity for 2−7 min, resulting in up to 53% reaction of the initial 1,3-butadiene. The concentrations of 1,3-butadiene and selected products were measured during the experiments by GC-FID. The concentrations of 1,3-butadiene were measured as described previously (*33*). For the analyses of reaction products, gas samples of 100 cm^3 volume were collected from the chamber onto Tenax-TA solid adsorbent with subsequent thermal desorption at ~225 °C onto a DB-1701 megabore column in a Hewlett-Packard (HP) 5710 GC, initially held at −40 °C and then temperature programmed to 200 °C at 8 °C min^{-1}. In addition, an Entech 7000 preconcentrator (Entech Instruments, Inc.) with a cold trap dehydration method was used to transfer gas samples collected from the chamber onto Tenax-TA solid adsorbent to a 30-m DB-1701 fused silica capillary column in an HP 5890 GC interfaced to a HP 5971A mass selective detector operating in the scanning mode for GC−MS analyses. GC-FID response factors were determined as previously described (*34*).

For the NO_3 radical reactions, NO_3 radicals were generated by the thermal decomposition of N_2O_5, and the initial 1,3-butadiene and NO_2 concentrations were $(5.7{-}6.0) \times 10^{13}$ and $\sim 4.8 \times 10^{13}$ molecule cm^{-3}, respectively. Three additions of N_2O_5 [corresponding to initial concentrations of N_2O_5 in the chamber of $(0.82{-}1.32) \times 10^{13}$ molecule cm^{-3}] were made to the chamber during an experiment. The concentrations of 1,3-butadiene and selected products were measured as described above.

Evacuable Chamber Experiments with FT-IR Analysis. Four OH radical reactions were carried out in the 5870-L evacuable, Teflon-coated chamber; two irradiations of $CH_3ONO{-}NO{-}$1,3-butadiene−air mixtures and two irradiations of $C_2H_5ONO{-}NO{-}$1,3-butadiene−air mixtures at 740 Torr total pressure and a relative humidity of <1%. The initial concentrations of the reactants were 2.46×10^{14} molecule cm^{-3} each. The irradiations were carried out intermittently with illumination periods of 0.5−1.25 min and total irradiation times of 5−6.5 min. IR spectra were recorded prior to the start of photolysis and during the intervening dark periods. Each spectrum was recorded with 64 scans (corresponding to 2.0-min averaging time), a full-width-at-half-maximum resolution of 0.7 cm^{-1}, and a path length of 62.9 m (*30, 34*). In one of the $CH_3ONO{-}NO{-}$1,3-butadiene−air irradiations, 4.9×10^{14} molecule cm^{-3} NO was added at the end of irradiation and monitored in the dark by FT-IR spectroscopy for 35 min.

Two NO_3 radical experiments were performed by adding N_2O_5, in aliquots of 2.46×10^{13} or 4.92×10^{13} molecule cm^{-3} to 2.46×10^{14} molecule cm^{-3} 1,3-butadiene in 740 Torr total pressure of air and by monitoring the reactants and products by FT-IR spectroscopy after each N_2O_5 addition. At the end of each of these two experiments, $(2.5{-}7.4) \times 10^{14}$ molecule cm^{-3} NO was added to the chamber, and the reactant mixtures monitored for 60 min. Because 1,3-butadiene reacts slowly with NO_2 in the dark (*20*), an experiment was also carried out to investigate this reaction by FT-IR spectroscopy with initial concentrations of NO_2 and 1,3-butadiene of 1.8×10^{14} and 2.46×10^{14} molecule cm^{-3}, respectively.

Teflon Chamber with Analysis by API-MS. In the experiments with API-MS analyses, the chamber contents were sampled through a 25 mm diameter × 75 cm length Pyrex tube at ~20 L min^{-1} directly into the API mass spectrometer source. The operation of the API-MS in the MS (scanning) and MS/MS [with collision activated dissociation (CAD)] modes has been described elsewhere (*35*). Use of the MS/MS mode with CAD allows the "daughter ion" or "parent ion" spectrum of a given ion peak observed in the MS scanning mode to be obtained (*35*). The positive ion mode was used in these API-MS and API-MS/MS analyses with protonated water hydrates ($H_3O^+(H_2O)_n$) generated by the corona discharge in the chamber diluent gas being responsible for the protonation of analytes. Ions are drawn by an electric potential from the ion source through the sampling orifice into the mass-analyzing first or third quadrupole. For these experiments, the API-MS instrument was operated under conditions that favored the formation of dimer ions in the ion source region (*35*). Neutral molecules and particles are prevented from entering the orifice by a flow of high-purity nitrogen (curtain gas), and as a result of the declustering action of the curtain gas on the hydrated ions, the ions that are mass-analyzed are mainly protonated molecular ions ($[M + H]^+$) and their protonated homo- and heterodimers (*35*).

For the OH radical reactions, the initial concentrations of CH_3ONO, NO, and 1,3-butadiene (or 1,3-butadiene-d_6) were $\sim 4.8 \times 10^{13}$ molecule cm^{-3} each, and irradiations were carried out for 2 min at 20% of the maximum light intensity. For the NO_3 radical reactions, the initial 1,3-butadiene (or 1,3-butadiene-d_6) and NO_2 concentrations were $\sim 4.8 \times 10^{13}$ molecule cm^{-3} each, and one addition of N_2O_5 (corresponding to an initial concentration of N_2O_5 in the chamber of $(2.2{-}3.9) \times 10^{13}$ molecule cm^{-3}) was made to the chamber during the experiment.

Chemicals. The chemicals used and their stated purities were as follows: acrolein (99+%), Aldrich Chemical Co.; 1,3-butadiene (≥99.0%), NO (≥99.0%), and NO_2 (≥99.5%), Matheson Gas Products; and 1,3-butadiene-d_6 (98%), Cambridge Isotope Laboratories. Methyl nitrite, ethyl nitrite, and N_2O_5 were prepared and stored as described previously (*29, 31, 34*).

Results

Gas Chromatographic Analyses. GC−MS and GC-FID analyses showed the formation of acrolein [$CH_2{=}CHCHO$] from both the OH and NO_3 radical reactions of 1,3-butadiene. Because acrolein also reacts with the OH radical, the measured acrolein concentrations in the OH radical-initiated reactions were corrected to take into account secondary reactions with the OH radical as described previously (*36*), using rate constants for the reactions of the OH radical with 1,3-butadiene and acrolein at 298 K of 6.66×10^{-11} and 1.99×10^{-11} cm^3 $molecule^{-1}$ s^{-1}, respectively (*20−22*). Corrections for secondary reactions of acrolein with the OH radical during the OH radical reactions were <14%. Corrections for the secondary reaction of acrolein with the NO_3 radical during the NO_3 radical reactions were negligible (<1%). The acrolein formation yields obtained from the OH and NO_3 radical-initiated reactions by least-squares analyses of the data obtained are given in Table 1.

Analyses by FT-IR Spectroscopy. *Reaction with the OH Radical.* The major products observed during the photolyses of $CH_3ONO{-}NO{-}$1,3-butadiene−air and $C_2H_5ONO{-}NO{-}$

TABLE 1. Products Identified and Their Formation Yields from the Reactions of 1,3-Butadiene with OH Radicals (in the Presence of NO) and NO_3 Radicals at 298 ± 2 K and Atmospheric Pressure of Air

product	formation yield GC-FID[a]	formation yield FT-IR[b]	formation yield literature	reference
		OH Radical Reaction		
acrolein	0.61 ± 0.05	0.55 ± 0.05	0.98 ± 0.12[c] ~0.39	Maldotti et al. (*23*) Ohta (*24*)
HCHO		0.62 ± 0.05		
furan		0.03−0.04[d]	0.060 ± 0.020 0.039 ± 0.011	Ohta (*24*) Atkinson et al. (*26*)
organic nitrates		0.07 ± 0.03[e]		
		NO_3 Radical Reaction [f]		
acrolein	0.039 ± 0.012	0.045	0.12 <0.05	Barnes et al. (*27*) Skov et al. (*28*)
HCHO		0.065	0.12 <0.05	Barnes et al. (*27*) Skov et al. (*28*)
furan		0.014		
organic nitrates		0.63 ± 0.15	~0.60	Barnes et al. (*27*)
$R(ONO_2)(OONO_2)$ species		0.08−0.16		

[a] Indicated errors are two least-squares standard deviations combined with the estimated overall uncertainties in the GC-FID response factors for 1,3-butadiene and acrolein of ±5% each. [b] Indicated errors are two least-squares standard deviations combined with the estimated overall uncertainties in the IR calibrations for 1,3-butadiene, HCHO, and acrolein of ±4, ±4, and ±5%, respectively. [c] As reevaluated by Atkinson (*22*). [d] Yield appeared to increase with the extent of reaction (see text). [e] The presence of high NO_2 concentrations during these reactions may result in this estimate of the organic nitrates yield being high (because of the occurrence of $R\dot{O} + NO_2$ reactions). [f] From experiments without addition of NO to reacted $N_2O_5-NO_3-NO_2-$1,3-butadiene−air mixtures.

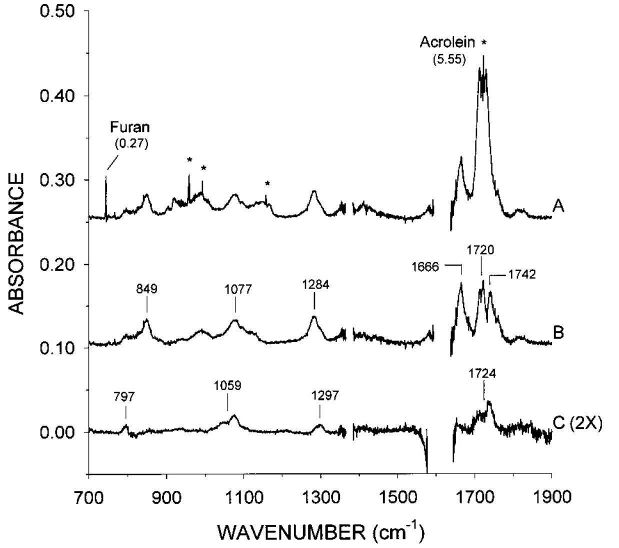

FIGURE 1. (A) Product spectrum from a 1,3-butadiene−CH_3ONO−NO−air photolysis after 6.5 min of irradiation and 1.10 × 10^{14} molecule cm^{-3} of 1,3-butadiene reacted (see text). (B) Residual spectrum from spectrum A after subtraction of absorptions by acrolein (noted by asterisks) and furan. (C) Difference between spectrum B and residual spectrum after addition of excess NO to the reaction mixture. Numbers in parentheses are concentrations in units of 10^{13} molecule cm^{-3}. (Gaps in the spectra in the 1615 and 1370 cm^{-1} regions correspond to strong absorptions by NO_2 formed and by the accumulated nitrate ions on the infrared windows, respectively.) The absorbances of spectra A and B are displaced vertically for clarity.

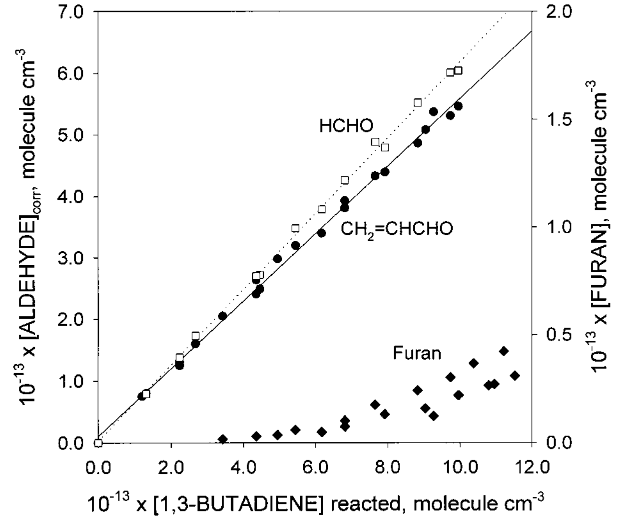

FIGURE 2. Plots of formaldehyde, acrolein, and furan formed against the amounts of 1,3-butadiene that reacted with OH radicals. The formaldehyde and acrolein concentrations were corrected for secondary reactions. Analyses were by FT-IR spectroscopy.

1,3-butadiene−air mixtures were acrolein and formaldehyde. Figure 1A shows infrared absorptions of acrolein among those of other products from irradiation of a $CH_3ONO-NO-$1,3-butadiene−air mixture after a total of 6.5 min of irradiation [the infrared absorptions of the remaining reactants, HCHO, and the other photooxidation products of CH_3ONO (CH_3ONO_2, HCOOH, NO_2, HNO_3, and HONO) have been subtracted]. The HCHO formation yields were determined from irradiations of $C_2H_5ONO-NO-$1,3-butadiene−air mixtures. Plots of the amounts of HCHO and acrolein formed, corrected for their reactions with OH radicals (*36*) using a rate constant for reaction of the OH radical with HCHO of 9.37 × 10^{-12} cm^3 $molecule^{-1}$ s^{-1} at 298 K (*22*), against the amounts of 1,3-butadiene reacted are presented in Figure 2, and their formation yields obtained from least-squares analyses of the data are given in Table 1. Corrections for secondary reactions with the OH radical were <9% for acrolein and <4% for HCHO.

Furan was observed as a minor product with its formation being indicated by the sharp Q-branch at 744.4 cm^{-1} in the product spectrum (Figure 1A). As shown by the data from four experiments plotted in Figure 2, the measured furan concentrations increased nonlinearly with the extent of irradiation, from being nondetectable after 1 min of photolysis to a yield of ~3−4% at the end of the 5−6.5-min total irradiation times. Other products that could be deduced from the residual spectrum shown in Figure 1B most likely contain C=O (~1720 and ~1742 cm^{-1}), OH (~1077 cm^{-1}), ONO_2 (1666,

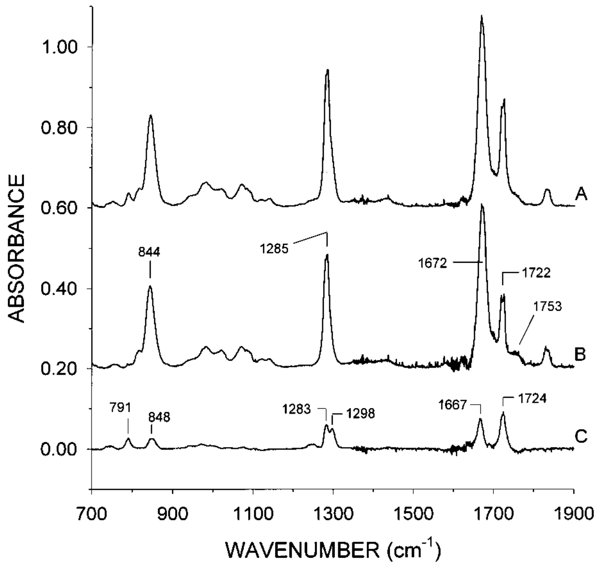

FIGURE 3. Product spectra from a reaction mixture of 1,3-butadiene and N_2O_5. (A) Residual spectrum depicting the major product(s) from 1.07 × 10^{14} molecule cm^{-3} of 1,3-butadiene consumed (see text). (B) Residual spectrum after addition of excess NO to the mixture. (C) Difference spectrum: spectrum A minus spectrum B. The absorbances of spectra A and B are displaced vertically for clarity.

1284, and 849 cm^{-1}), and $OONO_2$ (1724, 1297, and 797 cm^{-1}; see below) functional groups.

The total yield of products containing ONO_2 and $OONO_2$ groups was estimated to be 0.08 ± 0.03 based on the integrated area of the 1284 cm^{-1} band (Figure 1B) and an average integrated absorption coefficient of 1.3 × 10^{-17} cm molecule^{-1}. This average value was derived from measurements in this laboratory of the corresponding bands of CH_3ONO_2, $C_2H_5ONO_2$, $CH_3CH_2CH_2ONO_2$, and $CH_3C(O)OONO_2$, whose integrated absorption coefficients fall in the narrow range of (1.1−1.4) × 10^{-17} cm molecule^{-1} (*30*). The presence of a product containing an $OONO_2$ group was verified by the set of characteristic bands seen in Figure 1C (2× scale), which was obtained as the difference between the residual spectra at the end of irradiation (Figure 1B) and at 35 min after the addition of NO to the reaction mixture. No measurable loss of 1,3-butadiene accompanied the decomposition of the $ROONO_2$ product in the presence of excess NO. The intensity of the 1297 cm^{-1} peak in Figure 1C, a measure of the $ROONO_2$ formed, is a factor of ~8 lower than the overall integrated intensity of the 1284 cm^{-1} band in Figure 1B, and correction for this contribution leads to a yield estimate for the $RONO_2$ product of 0.07 ± 0.03. The presence of the 1059 cm^{-1} band in Figure 1C suggests that the $ROONO_2$ compound contains a hydroxyl group, and the possible presence of two overlapped bands in each of the regions around 1059 and 1724 cm^{-1} could indicate two positional isomers for the $ROONO_2$ formed. The occurrence of two distinct bands at ~1720 and ~1742 cm^{-1} in Figure 1B suggests the presence of two products containing a C═O group, with the lower frequency being most likely associated with a carbonyl compound containing a conjugated C═O group.

Reaction with the NO_3 Radical. The IR spectra obtained from reacting $N_2O_5-NO_3-NO_2$−1,3-butadiene−air mixtures showed that all of the N_2O_5 in each addition had reacted during the 3-min mixing time. Figure 3A depicts the absorption bands of the major product(s) after a total of 9.84 × 10^{13} molecule cm^{-3} of N_2O_5, in four equal aliquots, had been added to 2.46 × 10^{14} molecule cm^{-3} of 1,3-butadiene. A similar spectrum obtained 60 min after the addition of 2.46 × 10^{14} molecule cm^{-3} of NO to the above mixture is shown in Figure 3B. In Figure 3A,B, the absorption bands of the remaining 1,3-butadiene, NO_2, and observed minor products HCHO, acrolein, furan, HNO_3, and $HOONO_2$ (and NO in Figure 3B) have been subtracted. In Figure 3, subtraction of panel B from panel A resulted in panel C, which shows the presence of characteristic absorptions by an ONO_2 group at 1667, 1283, and 848 cm^{-1} and by an $OONO_2$ group at 1724, 1298, and 791 cm^{-1}, thus indicating the formation of an $R(ONO_2)(OONO_2)$-type compound that decomposed in the presence of excess NO. There was no significant difference in the integrated intensities of the 1285 cm^{-1} band between the spectra taken at 30 and 60 min after the addition of NO, and these intensities agreed, relative to the amount of 1,3-butadiene reacted, with those from a similar experiment where three times the above amount of NO was employed. This indicates that the amount of $R(ONO_2)(OONO_2)$ formed relative to the major ONO_2 group containing product(s) is fairly well approximated by Figure 3, panels C and B. However, the addition of NO after N_2O_5 had been consumed brought about further consumption of 1,3-butadiene. Thus, for example, in the experiment represented in Figure 3, 1.07 × 10^{14} molecule cm^{-3} 1,3-butadiene was consumed after the addition of N_2O_5, and an additional loss of 2.33 × 10^{13} molecule cm^{-3} 1,3-butadiene was recorded 60 min after the addition of NO to the reacted $N_2O_5-NO_2$−1,3-butadiene−air mixture.

The amount of ONO_2 group containing products was approximated from Figure 3B and similar spectra with the use of the 1285 cm^{-1} band (see the OH radical reaction above), resulting in an average molar yield of 0.63 from the two experiments that were conducted, relative to the amounts of 1,3-butadiene consumed prior to the addition of NO. This estimate includes any $RONO_2$ product(s) arising from $R(ONO_2)(OONO_2)$ decomposition [the formation of dinitrate products $R(ONO_2)(ONO_2)$ after decomposition of $R(ONO_2)(OONO_2)$ is expected to be minor (*20*)] and any $RONO_2$ formed from the additional 1,3-butadiene consumed after the addition of NO to the reacted $N_2O_5-NO_2$−1,3-butadiene−air mixture. Consideration of the reaction mechanisms involved (*20*) [see also Discussion below] suggests that the 1,3-butadiene consumed after NO addition is primarily due to reaction with OH radicals, in which case the ~7% yield of $RONO_2$ found in the OH radical reaction (see above) would translate to <3% contribution to the $RONO_2$ products represented in Figure 3B. On the assumption that the ONO_2 and $OONO_2$ groups of $R(ONO_2)(OONO_2)$ contribute additively (and equally) to the intensity of the ~1285 cm^{-1} absorption in Figure 3C, an average molar yield of 0.08 for $R(ONO_2)(OONO_2)$ is estimated from the two experiments. With the same assumption, a 1:1 conversion of $R(ONO_2)(OONO_2)$ to an $RONO_2$ product would then result in an intensity contribution to the ~1285 cm^{-1} band in Figure 3B, which is half that contributed by $R(ONO_2)(OONO_2)$ to the same band position in Figure 3A, and this leads to an upper-limit estimate of the $R(ONO_2)(OONO_2)$ formed being twice the 0.08 molar yield determined above. Hence, under the conditions of these experiments the actual yield of $R(ONO_2)(OONO_2)$ is probably in the range 0.08−0.16. Consideration of this uncertainty in the $R(ONO_2)(OONO_2)$ yield leads us to cite the organic nitrate yield as 0.63 ± 0.15.

The average molar formation yields of HCHO, acrolein, and furan from the two $N_2O_5-NO_2$−1,3-butadiene−air experiments obtained prior to the addition of NO were 0.065, 0.045, and 0.014, respectively. Therefore, prior to the addition of NO, the reaction of the NO_3 radical with 1,3-butadiene leads to the formation of HCHO, acrolein, furan, organic nitrates ($RONO_2$), and nitrooxy-peroxynitrates ($R(ONO_2)(OONO_2)$) with measured or estimated molar yields of 0.065, 0.045, 0.014, 0.63 ± 0.15, and 0.08−0.16, respectively. These products thus account for ~87 ± 16% of the total reaction

TABLE 2. Products Formed from the OH and NO_3 Radical-Initiated Reactions of 1,3-Butadiene And 1,3-butadiene-d_6 Using in Situ API-MS and API-MS/MS Analyses

reaction	products 1,3-butadiene	 1,3-butadiene-d_6
OH radical	acrolein (MW 56)	acrolein-d_4 (MW 60)
	$HOCH_2CH{=}CHCHO$ and isomers (MW 86)	$HOCD_2CD{=}CDCDO$ and isomers[a] (MW 91)
	$HOCH_2CH{=}CHCH_2ONO_2$ and isomers (MW 133)	$HOCD_2CD{=}CDCD_2ONO_2$ and isomers[b] (MW 139)
NO_3 radical	acrolein (MW 56)	acrolein-d_4 (MW 60)
	1,2-epoxy-3-butene (MW 70)	1,2-epoxy-3-butene-d_6 (MW 76)
	$HOCH_2CH{=}CHCHO$ and isomers (MW 86)	$HOCD_2CD{=}CDCDO$ and isomers[c] (MW 91)
	$O_2NOCH_2CH{=}CHCHO$ and isomers (MW 131)	$O_2NOCD_2CD{=}CDCDO$ and isomers (MW 136)
	$O_2NOCH_2CH{=}CHCH_2OH$ and isomers (MW 133)	$O_2NOCD_2CD{=}CDCD_2OH$ and isomers[c] (MW 139)
	$O_2NOCH_2CH{=}CHCH_2OOH$ and isomers (MW 149)	$O_2NOCD_2CD{=}CDCD_2OOH$ and isomers[c] (MW 155)

[a] Because rapid -OD to -OH exchange occurs under our experimental conditions, we cannot distinguish between reactions 9 and 10 as a formation route to this product. [b] Note that the H-atom in the -OH group arises from OH radical addition, and hence no -OD/-OH exchange occurred. [c] Rapid -OD to -OH exchange occurs under our experimental conditions.

products. The presence of a distinct absorption at 1722 cm^{-1} in Figure 3B indicates the presence of a C═O group, most likely conjugated, in the major $RONO_2$ product(s). The formation of other carbonyl products is not ruled out, including that indicated by a weak band envelope near 1753 cm^{-1}. The 1834 cm^{-1} band cannot be assigned to a plausible carbonyl product and is believed to be a combination band.

After addition of NO to these reacted $N_2O_5-NO_2-$1,3-butadiene−air mixtures, the HCHO, acrolein, and furan formation yields increased to 0.17, 0.13, and 0.059, respectively, relative to the overall amount of 1,3-butadiene consumed. The addition of NO to reacted $N_2O_5-NO_2-$1,3-butadiene−air mixtures leads to the decomposition of the $R(ONO_2)(OONO_2)$ compounds, with concurrent generation of OH radicals from the reactions of nitrooxyalkoxy radicals, $R(ONO_2)\dot{O}$, in the presence of NO (see Discussion below). Although, as discussed below, decomposition of $R(ONO_2)(OONO_2)$ species could form HCHO, acrolein, and furan, the additional amounts of HCHO and acrolein formed could be totally accounted for by assuming that all of the 1,3-butadiene consumed after the addition of NO was due to reaction with OH radicals, using the HCHO and acrolein yields (Table 1) obtained from CH_3ONO (or C_2H_5ONO)−NO−1,3-butadiene−air irradiations. Only a fraction of the additional furan formed could be accounted for by the ∼3−4% furan yield from the reaction of the OH radical with 1,3-butadiene, and most of the additional furan observed after the addition of NO must be formed from the reactions of $R(ONO_2)(OONO_2)$ and/or other undetermined products. If assumed as arising from the $R(ONO_2)(OONO_2)$ species, furan yields of 0.44 and 0.70 were calculated from the two experiments on the basis of the estimated $R(ONO_2)(OONO_2)$ yield of 0.08, and half of these formation yields if the $R(ONO_2)(OONO_2)$ yield was 0.16. The cause of the difference in the furan yields, after the addition of NO from the two experiments could not be determined.

Reaction with NO_2. A mixture of 2.46×10^{14} molecule cm^{-3} 1,3-butadiene in air with 1.8×10^{14} molecule cm^{-3} NO_2 resulted in a loss of ∼3% of the initial 1,3-butadiene after 90 min in the dark. The weak IR product spectrum showed that the product(s) formed contained both NO_2 (∼1360 and ∼1580 cm^{-1}) and ONO_2 (792, 1297, and 1725 cm^{-1}) groups. The slow reaction observed indicates that the extents of reaction of 1,3-butadiene with NO_2 in the OH and NO_3 radical-initiated reactions described above were negligible.

API-MS Analyses. API-MS/MS daughter ion and parent ion spectra were obtained for ion peaks observed in the API-MS analyses of the products of the reactions of OH radicals and NO_3 radicals with 1,3-butadiene and 1,3-butadiene-d_6. Product peaks were identified based on the observation of homo- or heterodimers (for example, $[(M_{P1})_2 + H]^+$, $[(M_{P2})_2 + H]^+$, and $[M_{P1} + M_{P2} + H]^+$, where P1 and P2 are products) in the API-MS/MS parent ion spectra and on consistency of the API-MS/MS daughter ion spectrum of a homo- or heterodimer ion with the parent ion spectra of the $[M_P + H]^+$ ion peaks (*35*). Water cluster ion peaks of the product ions, $[M + H + H_2O]^+$, were also observed in some instances.

The products observed from the reactions of 1,3-butadiene and 1,3-butadiene-d_6 with OH and NO_3 radicals are listed in Table 2. The evidence for the formation of these products, in the form of API-MS and API-MS/MS data of molecular ions, the dominant fragment ions, and the presence of homo- and heterodimers formed in the API-MS under the conditions used were obtained in a manner similar to previous product studies conducted in this laboratory (see, for example, ref *35*). In agreement with the GC and FT-IR analyses, acrolein (and acrolein-d_4) was observed as a product of both the OH and NO_3 radical reactions. In addition, $HOCH_2CH{=}CHCHO$ (and/or its isomers) and $HOCH_2CH{=}CHCH_2ONO_2$ (and/or its isomers) were observed as products of the OH radical with 1,3-butadiene, with the deuterated analogues being formed from the reaction of the OH radical with 1,3-butadiene-d_6. Representative API-MS/MS parent ion spectra are shown in Figures 4 and 5 for the OH radical reactions with 1,3-butadiene and 1,3-butadiene-d_6. These parent ion spectra demonstrate how evidence for the three products formed in the OH radical reaction was obtained, with homodimers of acrolein evident at 113 u in Figure 4A and homodimers of $HOCH_2CH{=}CHCHO$ (and/or its isomers of molecular weight 86) at 173 u in Figure 5A. The dimer ions in Figures 4A and 5A clearly show a total of three products with the molecular weight 133 species being attributed to $HOCH_2CH{=}CHCH_2ONO_2$ (and/or its isomers). The deuterated analogues in Figures 4B and 5B are consistent with these assignments, with the dimers shown in Figure 5B being dimers of $HOCD_2CD{=}CDCDO$ due to rapid D/H exchange for the alcohol if the initially formed species was $DOCD_2CD{=}CDCDO$ (see Discussion below). MS/MS spectra of the dimer peaks confirmed their identity.

The NO_3 radical reactions with 1,3-butadiene and 1,3-butadiene-d_6 each led to the formation of six products: these being acrolein, 1,2-epoxy-3-butene, $HOCH_2CH{=}CHCHO$, $O_2NOCH_2CH{=}CHCHO$, $O_2NOCH_2CH{=}CHCH_2OH$, and O_2-

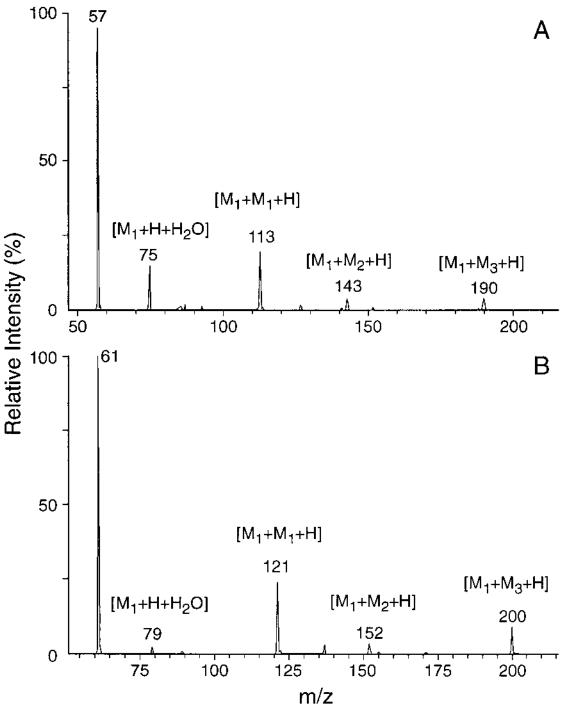

FIGURE 4. API-MS/MS CAD parent ion spectra of (A) the 57 u [M_1 + H]$^+$ ion observed in the API-MS spectrum of an irradiated CH_3-ONO−NO−1,3-butadiene−air mixture and (B) the 61 u [M_1 + H]$^+$ ion observed in the API-MS spectrum of an irradiated CH_3ONO−NO−1,3-butadiene-*d*$_6$−air mixture. The (unlabeled) ions peaks at 127 (A) and 137 u (B) are attributed to loss of HNO_3 from the 190 and 200 u dimer ions, respectively. M_1 is acrolein, M_2 is $HOCH_2CH{=}CHCHO$ and isomers, and M_3 is $HOCH_2CH{=}CHCH_2ONO_2$ and isomers. Note the increases in mass for the corresponding deuterated products shown in panel B (see Table 2 for details).

$NOCH_2CH{=}CHCH_2OOH$ (and/or their isomers) for the 1,3-butadiene reaction, and analogously for the 1,3-butadiene-*d*$_6$ reaction. Figure 6 shows the API-MS/MS daughter ion spectra of the [M + H]$^+$ ion peaks of the molecular weight 131 and 133 u products attributed to $O_2NOCH_2CH{=}CHCHO$ (and isomers) and $O_2NOCH_2CH{=}CHCH_2OH$ (and isomers), respectively (note the presence of intense 46 u [NO_2]$^+$ fragment ions and fragments corresponding to losses of HNO_3).

Of particular interest is that the API-MS/MS daughter ion spectra of the [M + H]$^+$ ions of the molecular weight 86 products from the 1,3-butadiene reactions with OH and NO_3 radicals are virtually identical (Figure 7) and similarly for the molecular weight 133 products. This is also the case for the API-MS/MS daughter ion spectra of the [M + H]$^+$ ions of the corresponding molecular weight 91 and 139 products from the 1,3-butadiene-*d*$_6$ reactions, as shown in Figure 8 for the 140 u [M + H]$^+$ ion peaks from the OH and NO_3 radical-initiated reactions. Thus, the dominant hydroxycarbonyl(s) and hydroxynitrate(s) from the OH and NO_3 radical reactions may be the same.

Discussion

OH Radical Reaction. The reaction of the OH radical with 1,3-butadiene proceeds by initial addition (*20*−*22*)

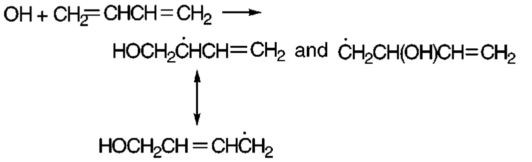

$$OH + CH_2{=}CHCH{=}CH_2 \longrightarrow HOCH_2\dot{C}HCH{=}CH_2 \text{ and } \dot{C}H_2CH(OH)CH{=}CH_2 \quad (5)$$
$$HOCH_2\dot{C}HCH{=}CH_2 \updownarrow HOCH_2CH{=}CH\dot{C}H_2$$

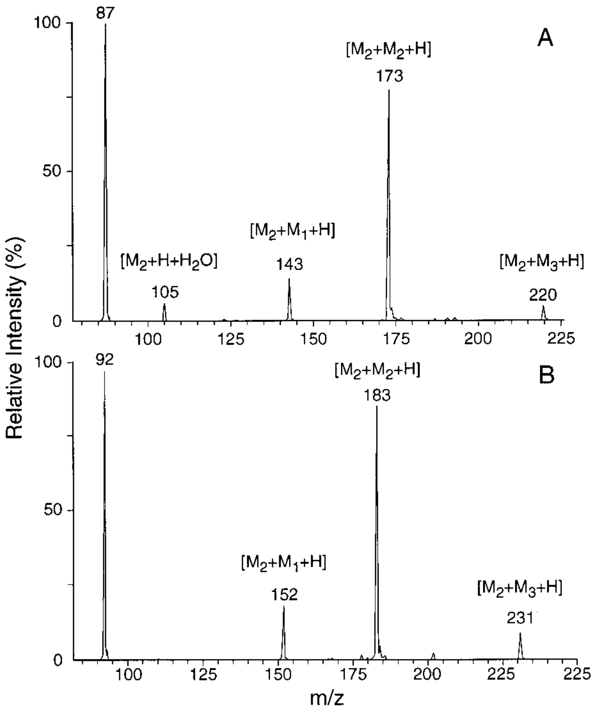

FIGURE 5. API-MS/MS CAD parent ion spectra of (A) the 87 u [M_2 + H]$^+$ ion observed in the API-MS spectrum of an irradiated CH_3-ONO−NO−1,3-butadiene−air mixture, and (B) the 92 u [M_2 + H]$^+$ ion observed in the API-MS spectrum of an irradiated CH_3ONO−NO−1,3-butadiene-*d*$_6$−air mixture. M_1, M_2, and M_3 are as given in the caption for Figure 4.

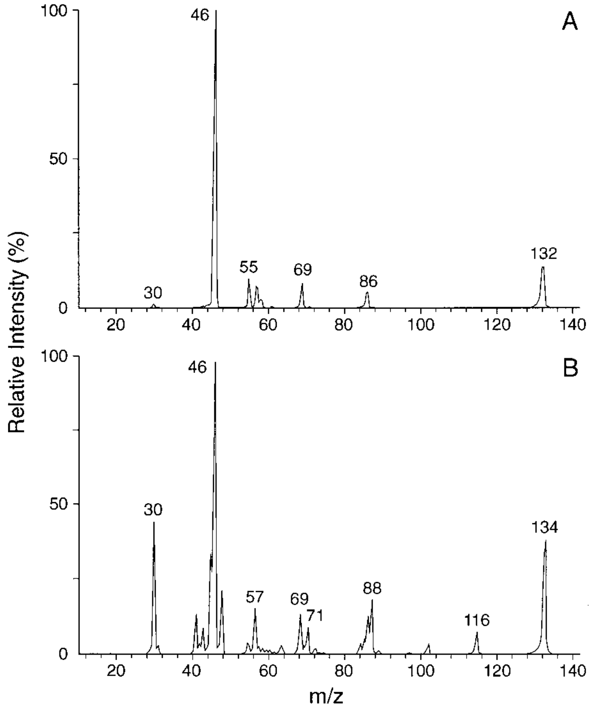

FIGURE 6. API-MS/MS CAD daughter ion spectra of (A) the 132 and (B) the 134 u ion observed in the API-MS spectra of reacted N_2O_5−NO_3−NO_2−1,3-butadiene−air mixtures. Fragment ions at 69 (A) and 71 u (B) are attributed to loss of HNO_3, and the 46 u fragment ions are attributed to NO_2^+. These spectra are attributed to protonated $O_2NOCH_2CH{=}CHCHO$ (A) and $O_2NOCH_2CH{=}CHCH_2OH$ (B) and/or their isomers.

leading, after addition of O_2, to the formation of the three hydroxyalkyl peroxy radicals $HOCH_2CH(\dot{O}O)CH{=}CH_2$, $CH_2{=}CHCH(OH)CH_2\dot{O}_2$, and $HOCH_2CH{=}CHCH_2\dot{O}_2$. In the pres-

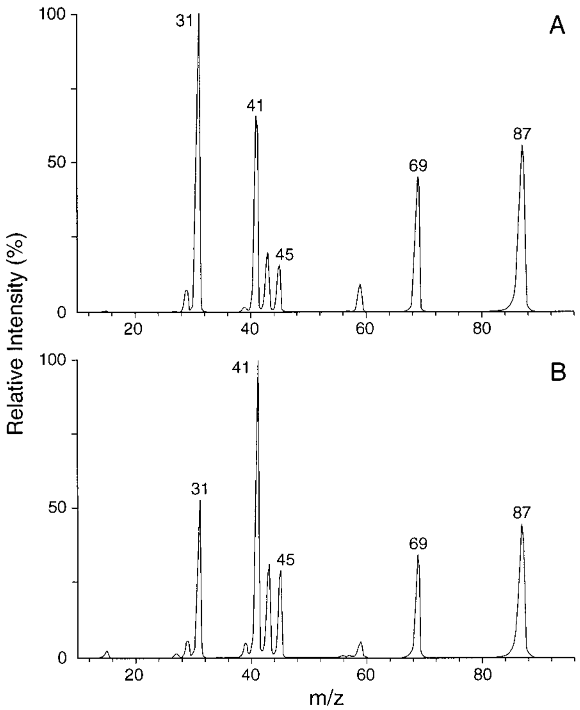

FIGURE 7. API-MS/MS CAD daughter ion spectra of the 87 u ions (attributed to protonated $HOCH_2CH{=}CHCHO$ and/or its isomers) observed in the API-MS spectra of (A) an irradiated $CH_3ONO-NO-$1,3-butadiene−air mixture and (B) a reacted $N_2O_5-NO_3-NO_2-$1,3-butadiene−air mixture.

ence of NO, these peroxy radicals react with NO to form either the corresponding hydroxyalkoxy radical plus NO_2 or the hydroxyalkyl nitrate. For example:

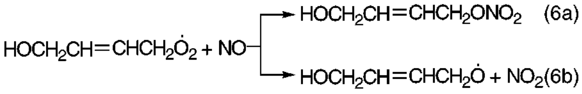

$$\mathrm{HOCH_2CH{=}CHCH_2\dot{O}_2 + NO \rightarrow HOCH_2CH{=}CHCH_2ONO_2} \qquad (6a)$$

$$\mathrm{HOCH_2CH{=}CHCH_2\dot{O}_2 + NO \rightarrow HOCH_2CH{=}CHCH_2\dot{O} + NO_2} \qquad (6b)$$

The resulting hydroxyalkoxy radicals $HOCH_2CH(\dot{O})CH{=}CH_2$, $CH_2{=}CHCH(OH)CH_2\dot{O}$, and $HOCH_2CH{=}CHCH_2\dot{O}$ can decompose, isomerize, or react with O_2 (*20*), with not all of these processes being possible for all three hydroxyalkoxy radicals formed from 1,3-butadiene. It is anticipated (*20*) that the $HOCH_2CH(\dot{O})CH{=}CH_2$ and $CH_2{=}CHCH(OH)CH_2\dot{O}$ radicals will primarily decompose

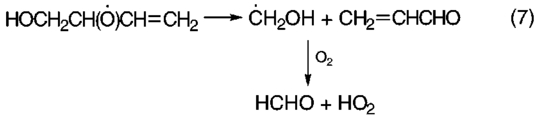

$$\mathrm{HOCH_2CH(\dot{O})CH{=}CH_2 \rightarrow \dot{C}H_2OH + CH_2{=}CHCHO} \qquad (7)$$
$$\mathrm{\dot{C}H_2OH \xrightarrow{O_2} HCHO + HO_2}$$

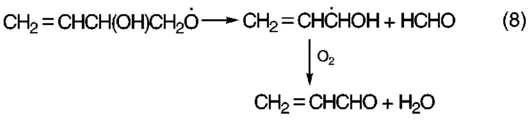

$$\mathrm{CH_2{=}CHCH(OH)CH_2\dot{O} \rightarrow CH_2{=}CH\dot{C}HOH + HCHO} \qquad (8)$$
$$\mathrm{CH_2{=}CH\dot{C}HOH \xrightarrow{O_2} CH_2{=}CHCHO + H_2O}$$

to form acrolein plus HCHO and that the $HOCH_2CH{=}CHCH_2\dot{O}$ radical will react with O_2 or isomerize (if conformationally possible)

$$\mathrm{HOCH_2CH{=}CHCH_2\dot{O} + O_2 \rightarrow HOCH_2CH{=}CHCHO + HO_2} \qquad (9)$$

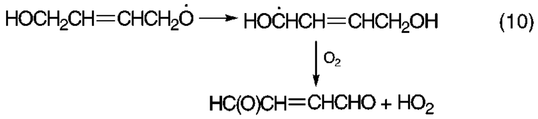

$$\mathrm{HOCH_2CH{=}CHCH_2\dot{O} \rightarrow HO\dot{C}HCH{=}CHCH_2OH} \qquad (10)$$
$$\mathrm{HO\dot{C}HCH{=}CHCH_2OH \xrightarrow{O_2} HC(O)CH{=}CHCHO + HO_2}$$

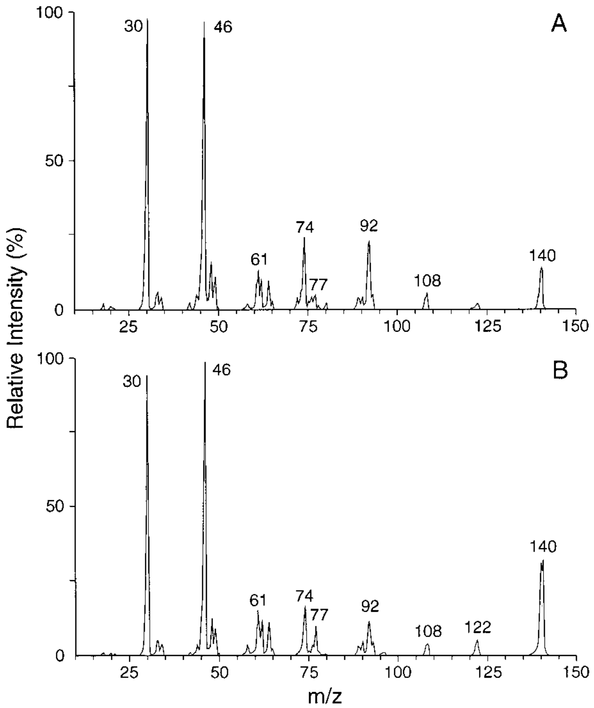

FIGURE 8. API-MS/MS CAD daughter ion spectra of the 140 u ions (attributed to protonated $HOCD_2CD{=}CDCD_2ONO_2$ and/or its isomers) observed in the API-MS spectra of (A) an irradiated $CH_3ONO-NO-$1,3-butadiene-d_6−air mixture and (B) a reacted $N_2O_5-NO_3-NO_2-$1,3-butadiene-d_6−air mixture. The fragment ions at 92 u are attributed to a loss of DNO_2.

SCHEME 1

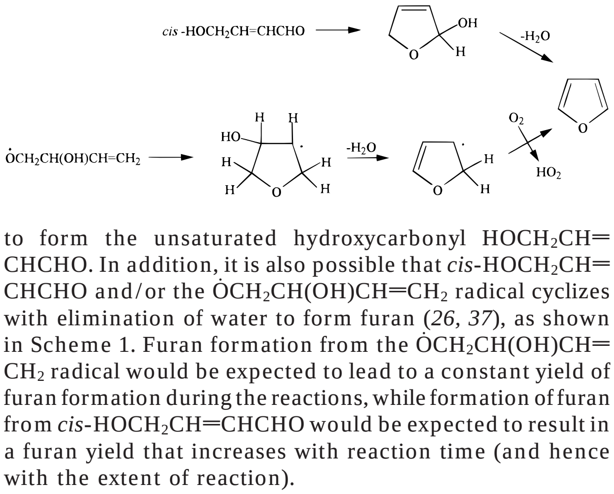

to form the unsaturated hydroxycarbonyl $HOCH_2CH{=}CHCHO$. In addition, it is also possible that *cis*-$HOCH_2CH{=}CHCHO$ and/or the $\dot{O}CH_2CH(OH)CH{=}CH_2$ radical cyclizes with elimination of water to form furan (*26*, *37*), as shown in Scheme 1. Furan formation from the $\dot{O}CH_2CH(OH)CH{=}CH_2$ radical would be expected to lead to a constant yield of furan formation during the reactions, while formation of furan from *cis*-$HOCH_2CH{=}CHCHO$ would be expected to result in a furan yield that increases with reaction time (and hence with the extent of reaction).

In the present study, acrolein, HCHO, and furan were identified and quantified by GC-FID and/or in situ FT-IR analyses (Table 1) with the formation yields of acrolein measured by GC-FID and by in situ FT-IR spectroscopy being in good agreement (Table 1). Furthermore, our measured formation yields for HCHO and acrolein are similar (Table 1), consistent with HCHO and acrolein being coproducts as expected from reactions 7 and 8. The slightly higher HCHO formation yield as compared to that of acrolein could arise from the formation of HCHO from secondary reactions of first-generation products, including from acrolein (*22*). Our API-MS and API-MS/MS analyses of the OH radical-initiated reactions of 1,3-butadiene and 1,3-butadiene-d_6 (Table 2) also indicated the formation of $HOCH_2CH{=}CHCHO$ (and/or its isomers) and $C_4H_7NO_4$ nitrates (for example, $HOCH_2CH{=}CHCH_2ONO_2$), and these API-MS and API-MS/MS analyses are substantiated by the FT-IR spectroscopic analyses that also show the formation of organic nitrates (Table 1) and provide confirmatory evidence for the presence of carbonyl compounds other than acrolein and HCHO.

The formation yields of acrolein and furan measured in previous literature studies (*23, 24, 26*) are also given in Table 1 for comparison with our present data. As evident from Table 1, our acrolein formation yield of 0.58 ± 0.04 (average of the GC-FID and FT-IR analyses) lies between the previous measurements of Maldotti et al. (*23*) and Ohta (*24*). In the study of Maldotti et al. (*23*), the acrolein formation yield was derived (*20, 22*) from the observation that the maximum concentration of acrolein in irradiated NO_x−1,3-butadiene−air mixtures was 59 ± 7% of the initial 1,3-butadiene concentration and the use of rate constants for the reactions of 1,3-butadiene and acrolein with the OH radical [making the reasonable assumption that the dominant loss process for both 1,3-butadiene and acrolein was by reaction with the OH radical (*22, 23*)]. The reasons for the discrepancies between our present study and those of Maldotti et al. (*23*) and Ohta (*24*) are not clear, but an acrolein formation yield of significantly less than unity is consistent with our API-MS and FT-IR analyses showing the formation of other products (namely $HOCH_2CH{=}CHCHO$, $HOCH_2CH{=}CHCH_2ONO_2$, and/or their isomers). Our present and previous (*26*) product formation yield data given in Table 1 combined with our API-MS and API-MS/MS analyses indicate that the reaction products are HCHO plus acrolein (58 ± 4%), furan (4 ± 1%), and organic nitrates (7 ± 3%; see footnote "e" in Table 1), with the remaining ~35% of the reaction products being attributed to the formation of the unsaturated hydroxycarbonyl $HOCH_2CH{=}CHCHO$ (and/or its isomers). Our investigation of the products and mechanism of the reaction of the OH radical with 1,3-butadiene indicates that the reaction mechanism is analogous to that of the corresponding reaction of the OH radical with isoprene (2-methyl-1,3-butadiene) (*20, 26, 30, 38*). Recently, Liu et al. (*25*) used a derivatization method, with *O*-pentafluorobenzylhydroxylamine as the derivatizing agent, to investigate the products of the NO_x−air photooxidation of 1,3-butadiene. A series of carbonyl-containing compounds were identified (or tentatively identified), including formaldehyde, acrolein (and its reaction products), and C_4-hydroxycarbonyl(s), as observed here. In addition, furan, 1,2-epoxy-3-butene, and 1,2,3,4-diepoxybutane were observed by gas chromatography (*25*).

It is interesting to note that we have previously observed that the formation yield of 3-methylfuran from the OH radical-initiated reaction of isoprene in the presence of NO was independent of the extent of reaction (*26*), in contrast to the data for furan formation from 1,3-butadiene shown in Figure 2. 3-Methylfuran has also been identified and quantified in ambient air collected at a rural forested site (*39*), and the 3-methylfuran and isoprene concentrations were consistent with the laboratory 3-methylfuran formation yield from isoprene (*26*), suggesting that in the isoprene system 3-methylfuran does not arise from C_5-hydroxycarbonyls [which are also isoprene reaction products (*38*)].

NO_3 Radical Reaction. The NO_3 radical reaction with 1,3-butadiene is analogous to the OH radical reaction in that the reaction proceeds by initial addition of the NO_3 radical to the carbon atoms of the >C═C< bonds (*20*). At low total pressures or in the absence of O_2, the resulting nitrooxyalkyl radical decomposes to NO_2 plus an oxirane. In the presence of O_2 (for example, in 1 atm of air), the thermalized nitrooxyalkyl radical reacts with O_2 to form the nitrooxyalkyl peroxy radical. Scheme 2 shows these reactions for the initial NO_3 radical addition to the 1-position in 1,3-butadiene. Therefore, in addition to the possible formation of 1,2-epoxy-3-butene, the nitrooxyalkyl peroxy radicals $O_2NOCH_2CH(\dot{O}O)CH{=}CH_2$, $CH_2{=}CHCH(ONO_2)CH_2\dot{O}_2$, and $O_2NOCH_2CH{=}CHCH_2\dot{O}_2$ are expected to be formed. In laboratory studies in the absence of added NO, $R\dot{O}_2 + NO_2$, $R\dot{O}_2 + R\dot{O}_2$ and $RO_2 + HO_2$ radical reactions occur (note that in the atmosphere it is probable that mainly $R\dot{O}_2 + HO_2$ radical reactions will occur) (*20, 22*). The reactions of the nitrooxyalkyl peroxy radicals with NO_2 lead to the formation of thermally unstable nitrooxyalkyl peroxynitrates, as, for example:

SCHEME 2

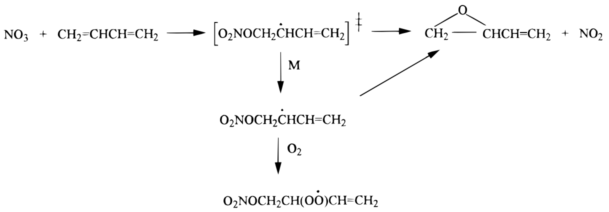

$$O_2NOCH_2CH{=}CHCH_2\dot{O}_2 + NO_2 \rightleftarrows O_2NOCH_2CH{=}CHCH_2OONO_2 \quad (11)$$

which act as a temporary reservior of $R\dot{O}_2$ radicals (see below). Taking the $O_2NOCH_2CH{=}CHCH_2\dot{O}_2$ radical as an example, the expected $R\dot{O}_2 + R\dot{O}_2$ and $RO_2 + HO_2$ radical reactions are as shown Scheme 3.

The other two nitrooxyalkyl peroxy radicals $O_2NOCH_2CH(O\dot{O})CH{=}CH_2$ and $CH_2{=}CHCH(ONO_2)CH_2\dot{O}_2$ will react by analogous reaction schemes with the nitrooxyalkoxy radicals formed being $CH_2{=}CHCH(\dot{O})CH_2ONO_2$ and $CH_2{=}CHCH(ONO_2)CH_2\dot{O}$. These two nitrooxyalkoxy radicals are expected to decompose or react with O_2, as for example

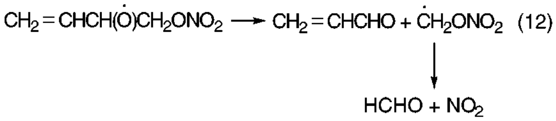

$$CH_2{=}CHCH(\dot{O})CH_2ONO_2 \rightarrow CH_2{=}CHCHO + \dot{C}H_2ONO_2 \quad (12)$$
$$\dot{C}H_2ONO_2 \rightarrow HCHO + NO_2$$

$$CH_2{=}CHCH(\dot{O})CH_2ONO_2 + O_2 \rightarrow CH_2{=}CHC(O)CH_2ONO_2 + HO_2 \quad (13)$$

The HO_2 radicals formed from these nitrooxyalkoxy radical reactions will react with NO, if added, to generate OH radicals:

$$HO_2 + NO \rightarrow OH + NO_2 \quad (14)$$

The products expected in the absence of added NO are therefore 1,2-epoxy-3-butene, HCHO + acrolein, $O_2NOCH_2CH{=}CHCHO$ and its isomers, $O_2NOCH_2CH{=}CHCH_2OH$ and its isomers, $O_2NOCH_2CH{=}CHCH_2OOH$ and its isomers, and $HOCH_2CH{=}CHCHO$. The addition of NO to reacting N_2O_5−NO_3−NO_2−1,3-butadiene−air mixtures converts nitrooxyalkyl peroxy radicals into the corresponding nitrooxyalkoxy radicals (and forms a small amount of dinitrate via reactions such as reaction 6a shown above for the OH radical-initiated reaction of 1,3-butadiene), with the nitrooxyalkoxy radicals expected to undergo decomposition, isomerization, or reaction with O_2 as shown in reactions 12 and 13 and Scheme 3.

For experiments carried out without addition of NO to the reactant mixtures, our GC-FID and in situ FT-IR analyses are in agreement with the previous studies of Barnes et al. (*27*) and Skov et al. (*28*) that formation of HCHO and acrolein is minor. The formation yields of acrolein measured here by GC-FID and FT-IR are in good agreement, and as shown in Table 1, our formation yields for HCHO and acrolein are reasonably consistent with the previous data of Barnes et al. (*27*) and Skov et al. (*28*). As may be expected, our IR spectra of the reaction products (Figure 3A) appears to be essentially identical to that presented by Skov et al. (*28*) [their Figure 1a], and the conclusions obtained from our FT-IR analyses are in accord with those of Barnes et al. (*27*) and Skov et al. (*28*) that the major products are organic nitrates. Thus, Barnes

SCHEME 3

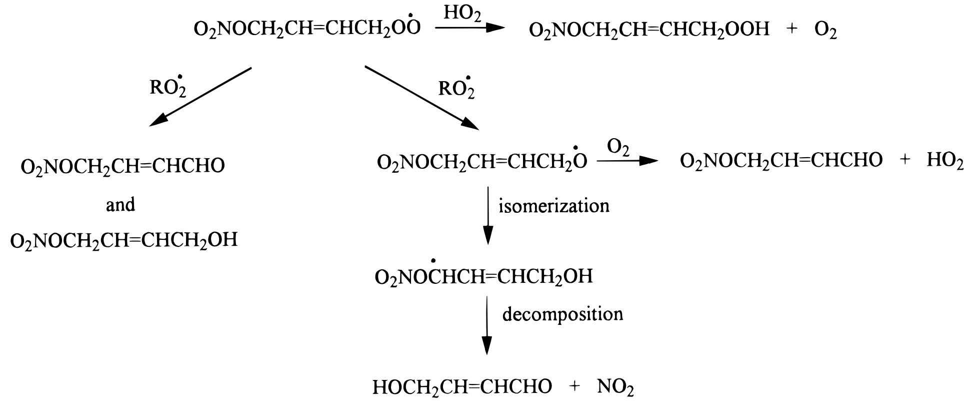

et al. (*27*) estimated that the yield of organic nitrates was ~60%, in agreement with our estimate of 63 ± 15% (Table 1), while Skov et al. (*28*) from their in situ FT-IR analyses and use of $LiAlH_4$ to reduce carbonyl (and nitrooxy) groups to hydroxyl groups concluded that the major products were *trans*-$O_2NOCH_2CH{=}CHCHO$ and $O_2NOCH_2C(O)CH{=}CH_2$, with *cis*-$O_2NOCH_2CH{=}CHCHO$ being formed in minor amounts.

Our API-MS and API-MS/MS analyses are generally consistent with the above FT-IR data from our study as well as Barnes et al. (*27*) and Skov et al. (*28*), showing the formation of acrolein, $HOCH_2CH{=}CHCHO$, $O_2NOCH_2CH{=}CHCHO$ (and/or its isomers), $O_2NOCH_2CH{=}CHCH_2OH$ (and/or its isomers) and $O_2NOCH_2CH{=}CHCH_2OOH$ (and/or its isomers), together with 1,2-epoxy-3-butene. The formation of these products is also consistent with the reaction schemes shown above, and the NO_3 radical-initiated reaction of 1,3-butadiene is then analogous to the corresponding NO_3 radical reactions with isoprene (*40*).

The addition of NO to reacting $N_2O_5{-}NO_3{-}NO_2{-}$1,3-butadiene−air mixtures under conditions such that an appreciable amount of the reacted 1,3-butadiene was present as the reservoir species nitrooxy-peroxynitrates [$R(ONO_2)(OONO_2)$ species] changed the product yields by significantly increasing the formation yields of HCHO, acrolein, and furan. The increased yields of HCHO and acrolein after NO addition are expected because the nitrooxyalkyl peroxy radicals are largely converted into nitrooxyalkoxy ($R\dot{O}$) radicals, which can then decompose, isomerize, or react with O_2, as shown in Scheme 3 and in reactions 12 and 13, to form at least in part, OH radicals that consume additional 1,3-butadiene. Indeed, as noted above the reactions of the OH radical with 1,3-butadiene can account for all of the additional HCHO and acrolein formed after NO addition. While formation of furan from the OH radical-initiated reaction of 1,3-butadiene has been postulated to occur from the cyclization of *cis*-$HOCH_2CH{=}CHCHO$ and/or the $\dot{O}CH_2CH(OH)CH{=}CH_2$ radical (*26, 37*) (Scheme 1), these processes are unlikely to account for the higher furan yields observed from the NO_3 radical-initiated reaction of 1,3-butadiene after the addition of NO. Although it is possible that the analogous cyclization of *cis*-$O_2NOCH_2CH{=}CHCHO$ and/or the $\dot{O}CH_2CH(ONO_2)CH{=}CH_2$ radical (with elimination of nitric acid) could occur (noting, however, that Skov et al. (*28*) observed *cis*-$O_2NOCH_2CH{=}CHCHO$, thus implying that not all *cis*-$O_2NOCH_2CH{=}CHCHO$ forms furan), the formation route(s) to furan formation in the NO_3 radical- (and OH radical) initiated reactions of 1,3-butadiene remains to be elucidated.

Clearly, further work is required to identify and quantify the specific isomeric products formed from both the OH and NO_3 radical-initiated reactions of 1,3-butadiene and to elucidate the reactions of nitrooxyalkoxy radicals formed as intermediates in the NO_3 radical-initiated reaction. However, it is also clear that multifunctional products are formed in large yield from these reactions; $HOCH_2CH{=}CHCHO$ (and/or its isomers) from the OH radical-initiated reaction and unsaturated C_4-hydroxycarbonyls, hydroxynitrates, carbonylnitrates, and nitrooxyhydroperoxides from the NO_3 radical-initiated reaction. Given the short lifetime of 1,3-butadiene in the atmosphere, these first-generation products are therefore expected to be present in the ambient atmosphere and to undergo further reactions.

Acknowledgments

The authors gratefully acknowledge the University of California Toxic Substances Research and Teaching Program and the U.S. Environmental Protection Agency, Office of Research and Development (Assistance Agreement R-825252-01-0) for support of this research. While this research has been supported in part by the U.S. Environmental Protection Agency, it has not been subjected to Agency review and therefore does not necessarily reflect the views of the Agency, and no official endorsement should be inferred.

Literature Cited

(1) Kao, A. S. *J. Air Waste Manage. Assoc.* **1994**, *44*, 683.
(2) *Proposed Update to the Toxic Air Contaminant List;* Draft Staff Report; Air Resources Board, California Environmental Protection Agency: Sacramento, CA, December 1998.
(3) Hoekman, S. K. *Environ. Sci. Technol.* **1992**, *26*, 1206.
(4) Barrefors, G.; Petersson, G. *J. Chromatogr.* **1993**, *643*, 71.
(5) Stump, F. D.; Knapp, K. T.; Ray, W. D.; Siudak, P. D.; Snow, R. F. *J. Air Waste Manage. Assoc.* **1994**, *44*, 781.
(6) Jemma, C. A.; Shore, P. R.; Widdicombe, K. A. *J. Chromatogr. Sci.* **1995**, *33*, 34.
(7) Kirchstetter, T. W.; Singer, B. C.; Harley, R. A.; Kendall, G. R.; Chan, W. *Environ. Sci. Technol.* **1996**, *30*, 661.
(8) Duffy, B. L.; Nelson, P. F. *Atmos. Environ.* **1996**, *30*, 2759.
(9) Stump, F. D.; Knapp, K. T.; Ray, W. D. *J. Air Waste Manage. Assoc.* **1996**, *46*, 1149.
(10) Ye, Y.; Galbally, I. E.; Weeks, I. A. *Atmos. Environ.* **1997**, *31*, 1157.
(11) Eatough, D. J.; Hansen, L. D.; Lewis, E. A. *Environ. Technol.* **1990**, *11*, 1071.
(12) Brunnemann, K. D.; Kagan, M. R.; Cox, J. E.; Hoffmann, D. *Carcinogenesis* **1990**, *11*, 1863.
(13) Matuška, P.; Koval, M.; Seiler, W. *J. High Resolut. Chromatogr., Chromatogr. Commun.* **1986**, *9*, 577.
(14) Kanakidou, M.; Bonsang, B.; Lambert, G. *Atmos. Environ.* **1989**, *23*, 921.
(15) Mowrer, J.; Lindskog, A. *Atmos. Environ.* **1991**, *25A*, 1971.
(16) Löfgren, L.; Petersson, G. *Sci. Total Environ.* **1992**, *116*, 195.
(17) Löfgren, L.; Petersson, G. *J. Chromatogr.* **1992**, *591*, 358.
(18) Boudries, H.; Toupance, G.; Dutot, A. L. *Atmos. Environ.* **1994**, *28*, 1095.

(19) Goldstein, A. H.; Daube, B. C.; Munger, J. W.; Wofsy, S. C. *J. Atmos. Chem.* **1995**, *21*, 43.
(20) Atkinson, R. *J. Phys. Chem. Ref. Data* **1997**, *26*, 215.
(21) Atkinson, R. *J. Phys. Chem. Ref. Data* **1989**, *Monogr. 1*, 1.
(22) Atkinson, R. *J. Phys. Chem. Ref. Data* **1994**, *Monogr. 2*, 1.
(23) Maldotti, A.; Chiorboli, C.; Bignozzi, C. A.; Bartocci, C.; Carassiti, V. *Int. J. Chem. Kinet.* **1980**, *12*, 905.
(24) Ohta, T. *Bull. Chem. Soc. Jpn.* **1984**, *57*, 960.
(25) Liu, X.; Jeffries, H. E.; Sexton, K. G. *Atmos. Environ.* **1999**, *33*, 3005.
(26) Atkinson, R.; Aschmann, S. M.; Tuazon, E. C.; Arey, J.; Zielinska, B. *Int. J. Chem. Kinet.* **1989**, *21*, 593.
(27) Barnes, I.; Bastian, V.; Becker, K. H.; Tong, Z. *J. Phys. Chem.* **1990**, *94*, 2413.
(28) Skov, H.; Hjorth, J.; Lohse, C.; Jensen, N. R.; Restelli, G. *Atmos. Environ.* **1992**, *26A*, 2771.
(29) Atkinson, R.; Carter, W. P. L.; Winer, A. M.; Pitts, J. N., Jr. *J. Air Pollut. Control Assoc.* **1981**, *31*, 1090.
(30) Tuazon, E. C.; Atkinson, R. *Int. J. Chem. Kinet.* **1990**, *22*, 1221.
(31) Atkinson, R.; Plum, C. N.; Carter, W. P. L.; Winer, A. M.; Pitts, J. N., Jr. *J. Phys. Chem.* **1984**, *88*, 1210.
(32) Atkinson, R.; Aschmann, S. M.; Pitts, J. N., Jr. *J. Phys. Chem.* **1988**, *92*, 3454.
(33) Atkinson, R.; Aschmann, S. M. *Environ. Sci. Technol.* **1993**, *27*, 1357.
(34) Atkinson, R.; Tuazon, E. C.; Aschmann, S. M. *Environ. Sci. Technol.* **1995**, *29*, 1674.
(35) Aschmann, S. M.; Chew, A. A.; Arey, J.; Atkinson, R. *J. Phys. Chem. A* **1997**, *101*, 8042.
(36) Atkinson, R.; Aschmann, S. M.; Carter, W. P. L.; Winer, A. M.; Pitts, J. N., Jr. *J. Phys. Chem.* **1982**, *86*, 4563.
(37) Gu, C.-L.; Rynard, C. M.; Hendry, D. G.; Mill, T. *Environ. Sci. Technol.* **1985**, *19*, 151.
(38) Kwok, E. S. C.; Atkinson, R.; Arey, J. *Environ. Sci. Technol.* **1995**, *29*, 2467.
(39) Montzka, S. A.; Trainer, M.; Angevine, W. M.; Fehsenfeld, F. C. *J. Geophys. Res.* **1995**, *100*, 11393.
(40) Kwok, E. S. C.; Aschmann, S. M.; Arey, J.; Atkinson, R. *Int. J. Chem. Kinet.* **1996**, *28*, 925.

Received for review February 17, 1999. Revised manuscript received June 24, 1999. Accepted July 21, 1999.

ES990193U